System Identification of Space Structures[1]

Seth L. Lacy[2] Vit Babuška[3] Karl N. Schrader[4] Robert Fuentes[5]

Abstract— **Large precision spacecraft present a challenging control problem. They are modally dense, have a very large frequency bandwidth over which disturbances can affect payload performance, and are lightly damped. The performance of passive vibration isolation systems will be limited by the constraints of physics and mechanical components, particularly at low frequencies. This motivates the need for an active isolation system. High fidelity system models are required to obtain the high performance control. Developing these high fidelity system models of large space structures is a challenge for experiments, algorithms, and computational resources.**

I. Introduction

The Air Force Research Laboratory's Deployable Optical Telescope (DOT) is a space traceable sparse-aperture telescope with deployable primary and secondary mirrors developed under the Large Deployable Optics program, see Figures 1 and 2. This laboratory experiment is being used to develop and evaluate technologies critical to the fielding of future large space telescopes. It is necessary to control the position of the three-segment primary mirror in order to correct for deployment errors, ambient disturbances, and persistent disturbance sources traceable to spacecraft subsystems associated with attitude control and thermal management. Our work has focused on obtaining linear models of large space structures using both time [17] and frequency domain subspace methods [8, 10–12], leading to several challenges for data collection and linear system identification algorithm implementation. Subspace methods are attractive for high bandwidth identification of lightly damped, modally dense structures. They are numerically robust and efficient.

This tutorial is based on our experiences developing data-based models of the DOT using implementations of subspace system identification algorithms available in commercial tools. For the frequency domain identification, the FORSE (Frequency Domain Observability Range Space Extraction) method [8, 10] as implemented in the DynaMod package [2] is being used. For time domain identification, the CVA (Canonical Variate Analysis) algorithm as implemented in the AdaptX package [9] was tested.

II. Experiment Description and Approach

The DOT (Deployable Optical Telescope) shown in Figures 1 and 2 is a space-traceable telescope. The primary mirror segments and secondary mirror tower each contain deployment mechanisms. The primary mirror deployment mechanisms are hinges and latches. The secondary mirror tower is deployed linearly and latched into place. This allows for a large telescope to be launched in a small volume. The secondary mirror is mounted on a hexapod capable of positioning the mirror in six degrees of freedom to correct for static deployment errors. The first few structural modes associated with the secondary mirror tower are weakly controllable from the primary mirror actuators. An additional piezo patch actuator system is bonded to the base of the tower to control these structural modes. The

Fig. 1. The Deployable Optical Telescope

[1]This work was supported in part by the AFOSR under laboratory research initiative 00VS17COR.

[2]Air Force Research Laboratory, seth.lacy@kirtland.af.mil
[3]General Dynamics AIS, vit.babuska@kirtland.af.mil
[4]Boeing SVS, karl.schrader@kirtland.af.mil
[5]Boeing SVS, robert.fuentes@kirtland.af.mil

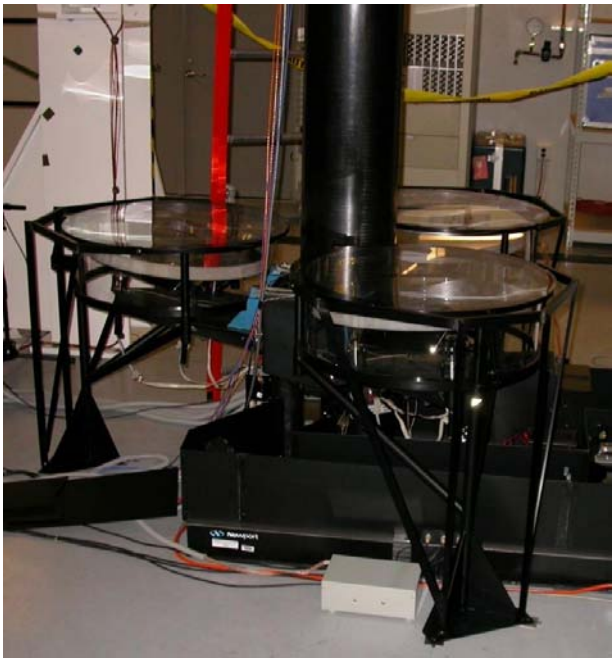

Fig. 2. The Deployable Optical Telescope with mirror covers

three primary mirror segments are each actuated in three degrees of freedom and are actively controlled to correct for dynamic motion of the optical support structure. The position of each of the three primary mirror segments is measured in three degrees of freedom: piston, tip, and tilt. In total, there are 10 actuators (three for each primary mirror and one for the secondary mirror support tower) and 9 sensors (three for each primary mirror). More information on the experiment design, construction, and control can be found in [1, 4, 5, 7, 13–15].

The Large Deployable Optics team has focused on collecting input-output data in the time and frequency domain for system identification. There are advantages and disadvantages to working in each domain. Frequency domain data can be very efficient. Each data point in the frequency domain may be the result of significantly averaged time domain data. In the frequency domain, the input sequence used to excite the system can easily be tailored to the dynamics of the plant. This allows us to excite the system at high levels where the system has low response and at low levels where the system has high response. The drive signal can also be constructed to maximize the amount of energy at the frequencies of interest and to minimize the wasted energy applied at other frequencies. In the time domain, the data can be collected from all actuators at once, decreasing the experiment duration required to collect the data.

III. Data Collection

Data collection has become an important aspect of this experiment. Improved methods for data collection are actively being researched, and are described here. In the frequency domain, we tested several excitation signals. For each type, the input was applied to one actuator at a time, while monitoring all sensors. This data was processed to estimate the frequency response function for each input-output pair. These individual channel frequency response functions were then combined to produce the frequency response matrix for the system. This matrix is the input to the frequency domain system identification methods. In the time domain, we tested random input sequences.

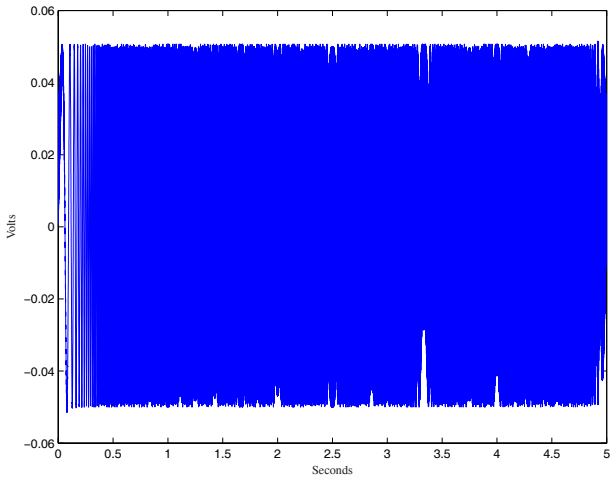

Fig. 3. Schroeder phase input sequence with content from 0-1000Hz and 1/5 Hz resolution

A. Frequency Domain: Random

A random input signal was inefficient for developing frequency domain data. Due to saturation constraints on the input magnitude, the resulting signal to noise ratio is severely limited over the broad frequency band of interest. Although better SNR could be achieved by coloring the input signal, at this moment there is no plan to conduct such tests. Data averaging would not be appropriate for zero mean input sequences, although averaging in the spirit of [6] is possible.

B. Frequency Domain: Schroeder Phase

A Schroeder phase input sequence [16] was also implemented, see Figure 3. The Schroeder phase input sequence is a sum of sinusoids with their phases chosen to minimize the peak amplitude of the signal. This input signal has several advantages. It has a flat power spectrum, see Figure 4 (the minimum and maximum levels are actually -59.030900 dB/Hz and -59.030899 dB/Hz). It is a deterministic signal, and can be applied repeatedly and the responses averaged to reduce the effect of disturbances present in the laboratory.

During our data collection efforts, we investigated the effect that input sequence amplitude had on the estimated frequency response function. Figure 5 shows the frequency response function estimate and the coherence using an input sequence amplitude of 0.05 Volts. The frequency response and coherence measured with an input amplitude of 3.0 Volts is shown in Figure 6 Ideally, these two estimates

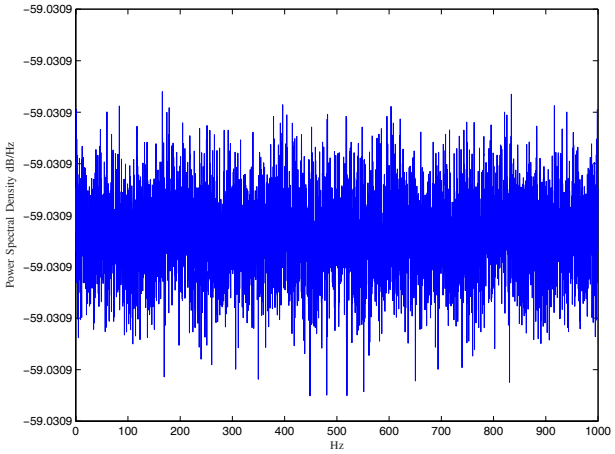

Fig. 4. Power Spectrum of a Schroeder phase input sequence with content from 0-1000Hz and 1/5 Hz resolution

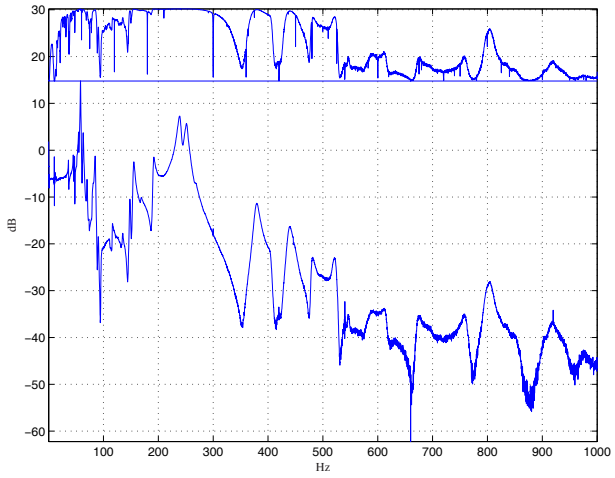

Fig. 5. Frequency response of $G(2,1)$ with low amplitude input

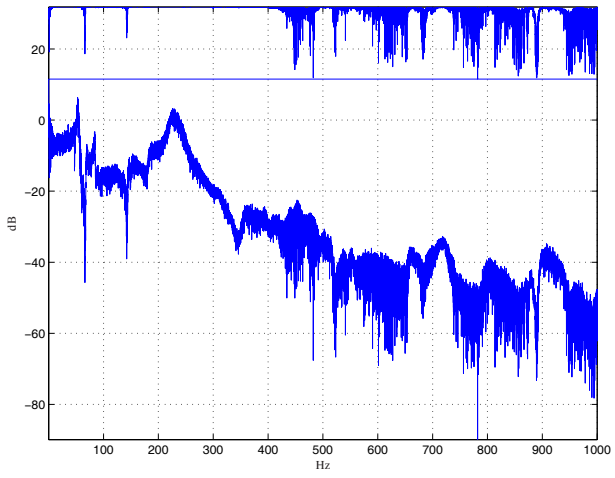

Fig. 6. Frequency response of $G(2,1)$ with high amplitude input

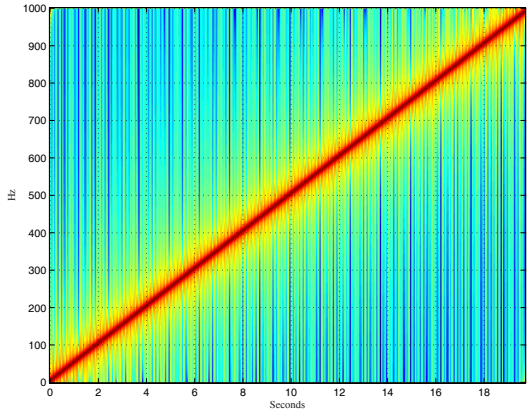

Fig. 7. Specgram of the input sequence

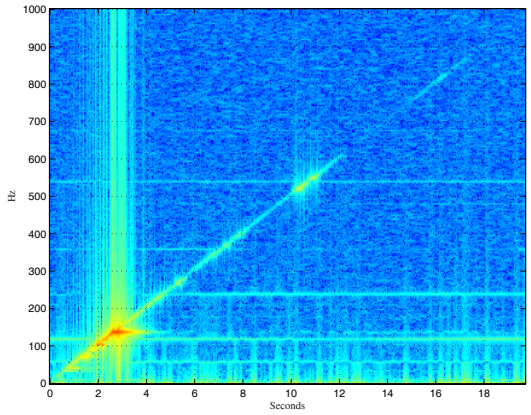

Fig. 8. Specgram of the output sequence corresponding to an input amplitude of 0.05 V

would agree. While the coherence of the high amplitude data is much better (closer to 1) than the coherence of the low amplitude data, the high amplitude frequency response function does not qualitatively "look" better than the low amplitude frequency response function.

We plotted specgram's of the data to investigate this issue. A specgram plot is a running plot of the power spectral density of a signal. Figure 7 shows the specgram of the input sequence. The frequency content of the input sequence changes from low frequency to high frequency as the signal evolves in time, characteristic of a chirp. The responses from the low and high amplitude input sequences are shown in Figures 8 and 9. The harmonics present in the high amplitude data are clearly visible. This suggests that there are amplitude dependant nonlinearities in the system. Further investigation revealed that the amplifiers used to drive the piezo actuators were unable to deliver the large power spikes resulting from the zero-order-held command sequence. To alleviate this problem, the input sequence is now low-pass-filtered prior to going to the piezo amplifiers.

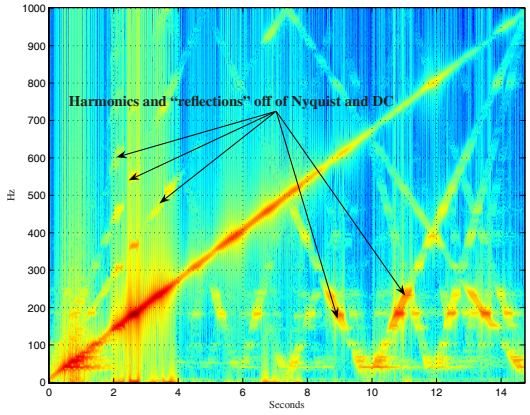

Fig. 9. Specgram of the output sequence corresponding to an input amplitude of 3 V

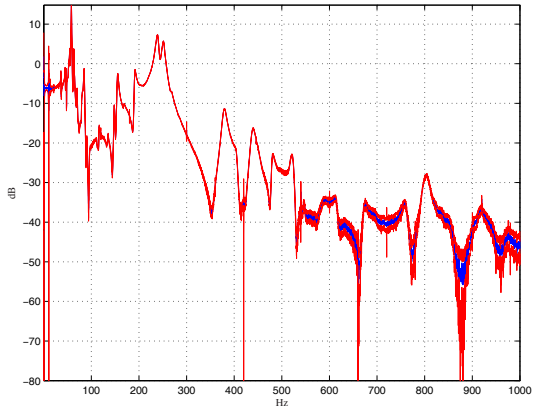

Fig. 10. Frequency response of $G(2,1)$ with 99% confidence interval

This introduces some phase lag, but eliminates much of the nonlinear response visible in the specgram due to the amplifier saturation.

To evaluate the quality of the estimated frequency response functions we computed 99% confidence disks around each complex point in the frequency response, see Figure 10. The principal gains of the frequency response function matrix are shown in Figure 11.

The deterministic nature of the Schroeder Phase input sequence and the remaining nonlinearity in the system make this data collection technique unsuitable for our purposes. The harmonics generated at a resonance are large compared to areas of low response. A harmonic, or it's Nyquist-folded effective frequency, that coincides with an area of low response for an input-output pair can create undesired artifacts in the frequency response, see Figure 12. Because of the deterministic nature of the Schroeder Phase input sequence, the effect of these harmonics are not reduced with data averaging.

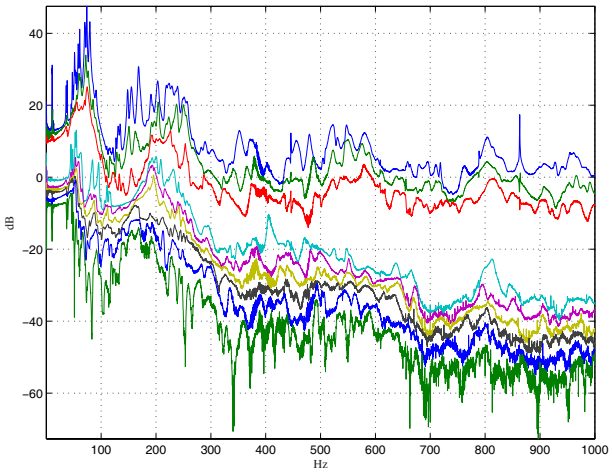

Fig. 11. Principal gains of the measured Schroeder phase data

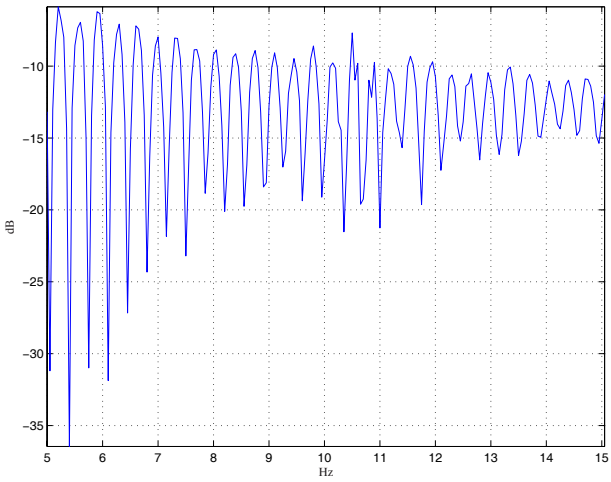

Fig. 12. An example of nonlinearity induced artifacts in a Schroeder phase derived FRF

C. Frequency Domain: Sine Dwell

We were driven to sine dwell testing to collect data for our frequency domain system identification techniques. The drawback to this method of data collection is that the required test duration can be extremely long. The advantages are

1) We have complete insight in to the nonlinearity generated harmonics at each frequency.
2) We can tailor the duration of the sinusoid at each frequency to the disturbance environment of the plant.
3) We can tailor the amplitude of the sinusoid at each frequency to the disturbance environment and response of the plant.
4) Uncertainty information is readily calculated.
5) Variable frequency spacing can be used to gather more data in areas of interest and to reduce the

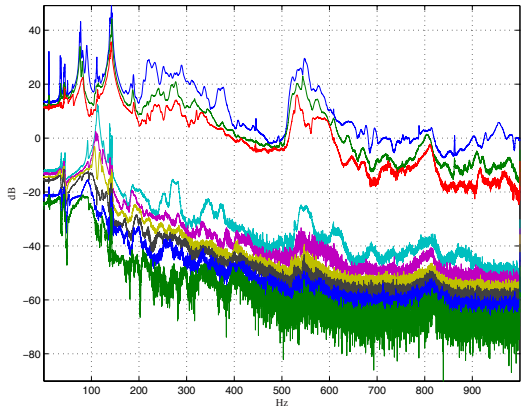

Fig. 13. Principal gains of the sine dwell data

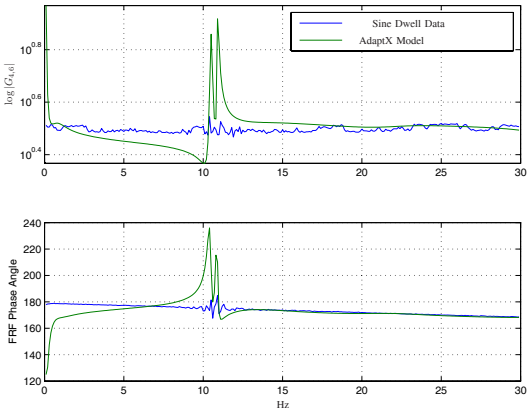

Fig. 14. CVA model and sine dwell data near 10Hz

data collection time in other areas. Interpolation can be used to generate a uniform frequency spacing if required.

We estimated the frequency response for each input-output pair, and combined these individual channel FRF's into the FRF matrix for the system, see Figure 13.

D. Time Domain: Random

We applied random input sequences to all 10 actuators simultaneously and measured all 9 sensors. The sequence applied to each channel is uncorrelated with the input sequence applied to other channels. Deterministic input sequences would have to be chosen carefully. We thus used a random sequence for each of the 10 input channels. This random data was then used for model development.

IV. System Identification

We applied time and frequency domain methods to data collected in the previous section.

A. System Identification: Time Domain

We applied the method of [9] and identified a model with 200 lags, and 644 states. This application exposed one serious constraint of time domain methods in general for application to lightly damped systems under the influence of disturbances. The number of lags used is limited to around 200 by the memory constraints of the computer used for this analysis (4GB). For short data lengths, the response of the two modes near 10Hz due to the ambient disturbance environment is difficult to separate from the response due to the commanded input. The time domain identified model indicates that these two modes are controllable from several actuators, while the sine dwell data collected using 100,000 samples reveals that these actuators do not in fact have authority over these two system modes. See Figure 14. This computational restriction on the number of lags makes this approach unsuitable for our application. Future development of memory-conservative time domain system identification algorithms may alleviate this difficulty. Data compression methods [6] may also be suitable for this application.

B. System Identification: Frequency Domain

We have used the frequency domain system identification tool Dynamod [2] on several projects with good results. For more details on frequency domain system identification algorithms see [2, 8, 11]. Using the software tool, the modeler can add and remove dynamics from the model, as well as tune the model using an iterative search algorithm based on several model fit metrics with frequency weighting. The numerical value of some measurement channels is smaller than others. The result of this is that the high response channels are fit better than the low response channels. To correct this scaling issue, we applied weighting matrices to the data as

$$G_{id}(\omega) = W_o G_{data}(\omega) W_i \tag{4.1}$$

where G_{id} is the data used for identification, W_o is the output weighting matrix, G_{data} is the measured frequency response data, and W_i is the input weighting matrix. The weighting matrices were chosen to emphasize the channels with small units as compared to the channels with large units. The singular values of the (un-weighted) model are shown in Figure 15. The principal gain of the model, the principal gain of the data, and the principal gain of the error between the model and the data are shown in Figure 16.

V. Control Design

The baseline control approach is a gain-scheduled linear optimal control design based on [3]. Additional options for control design are currently being assessed. Integrator states are included to drive the measured outputs to the desired set points. A complication is that the interferometer measurements that are used to measure the piston displacement of each primary mirror segment are somewhat unreliable. The interferometer will occasionally "lose lock". Fortunately, this sensor failure does not affect the underlying dynamics of the plant. We have tackled this problem using

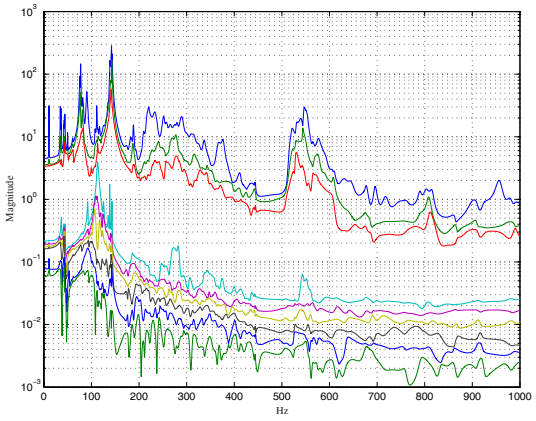

Fig. 15. Principal gains of the model

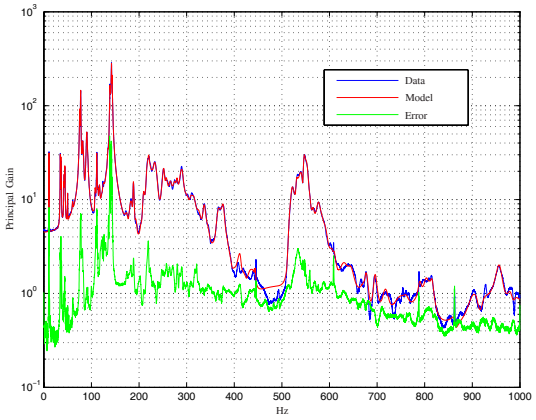

Fig. 16. Principal gain of the data, model, and the error

state estimators designed for every combination of possible sensor failures. These estimators are switched between based on which sensors are reading valid data. Previous implementations of this control approach on the DOT are described in [5, 13, 14].

VI. Summary

We described our experience in applying different system identification techniques for linear systems to a space-traceable testbed. Computational constraints restricted us to frequency domain techniques. Nonlinear response in the system drove us to use sine dwell data collection techniques. We constructed high fidelity models of the system suitable for control design using sine dwell data collection and frequency domain system identification techniques.

VII. Conclusion

Large space structures present a challenging system identification problem. They are modally dense, have a very large frequency bandwidth over which disturbances can affect payload performance, and are lightly damped. High fidelity system models are required to obtain high performance control. Frequency domain algorithms are currently the most suitable for application to these problems due to limited existing computational resources and ambient disturbances coupling with the lightly damped structural resonances. Experimental conditions may dictate the use of time consuming data collection techniques.

Future efforts will focus on control and performance. Wavefront reconstruction techniques will be applied and integrated with the existing high-bandwidth control. Finally, we will investigate uncertainty quantification in all stages of the process: data collection, system identification, control design, and ultimate performance prediction.

References

[1] K. D. Bell, R. L. Moser, M. K. Powers, and S. R. Erwin, "Deployable optical telescope ground demonstration," in *Proceedings of the SPIE*, Munich Germany, July 2000, pp. 559–567.

[2] C. Blaurock, *Dynamod Users Manual*, Midé Technology Corporation, 200 Boston Ave, Suite 1000, Medford, MA 02155, 2003.

[3] P. Dorato, C. Abdallah, and V. Cerone, *Linear Quadratic Control, An Introduction*. Krieger Publishing Company, July 2000.

[4] R. S. Erwin, K. N. Schrader, R. L. Moser, and S. F. Griffin, "Experimental demonstration of precision control of a deployable optics structure," *Journal of Vibration and Acoustics*, vol. 124, no. 3, pp. 441–450, July 2002.

[5] R. J. Fuentes, K. N. Schrader, M. J. Balas, and R. S. Erwin, "Direct adaptive disturbance rejection and control for a deployable space telescope, theory and application," in *American Control Conference*, Arlington VA, June 2001, pp. 3980–3985.

[6] I. I. Hussein, S. L. Lacy, and D. S. Bernstein, "Data compression for subspace-based identification using periodic inputs," in *Proceedings of the American Control Conference*, Anchorage, Alaska, May 2002.

[7] S. Huybrechts, P. Wegner, A. Maji, B. Kozola, S. Griffin, and T. Meink, "Structural design for deployable optical telescopes," in *2000 IEEE Aerospace Conference Proceedings*, Big Sky, MT, March 2000, pp. 367–372.

[8] R. N. Jacques, K. Liu, and D. W. Miller, "Identification of highly accurate low order state space models in the frequency domain," *Signal Processing*, vol. 52, no. 2, pp. 195–207, July 1996.

[9] W. E. Larimore, ADAPT$_X$ *Users Manual*, Adaptics, Inc, McLean VA, 1999.

[10] K. Liu, R. N. Jacques, and D. W. Miller, "Frequency domain structural system identification by observability range space extraction," *Journal of Dynamic Systems Measurement and Control*, vol. 118, pp. 211–220, 1996.

[11] T. McKelvey, H. Akçay, and L. Ljung, "Subspace-based identification of infinite-dimensional multivariable systems from frequency-response data," *Automatica*, vol. 32, no. 6, pp. 885–902, June 1996.

[12] R. Pintelon and J. Schoukens, *System Identification: A Frequency Domain Approach*. Piscataway, NJ: IEEE Press, 2001.

[13] K. N. Schrader, R. H. Fetner, M. J. Balas, and S. R. Erwin, "Sparse-array phasing algorithm based on recursive estimation of fringe contrast," in *Proceedings of the SPIE*, Waikoloa, HI, August 2002, pp. 146–157.

[14] K. N. Schrader, R. H. Fetner, J. H. Donaldson, R. J. Fuentes, and S. R. Erwin, "Integrated control system development for phasing and vibration suppression for a sparse-array telescope," in *Proceedings of the SPIE*, Waikoloa, HI, August 2002, pp. 134–135.

[15] K. N. Schrader, R. H. Fetner, S. F. Griffin, and S. R. Erwin, "Development of a sparse-aperture testbed for opto-mechanical control of space-deployable structures," in *Proceedings of the SPIE*, Waikoloa, HI, August 2002, pp. 384–395.

[16] M. R. Schroeder, "Synthesis of low-peak-factor signals and binary sequences with low autocorrelation," *IEEE Transactions on Information Theory*, vol. 16, no. 1, pp. 85–89, January 1970.

[17] P. Van Overschee and B. De Moor, *Subspace Identification for Linear Systems: Theory, Implementation, Applications*. Kluwer, 1996.